Biological Hip Torque Estimation using a Robotic Hip Exoskeleton

Dean D. Molinaro, *Student Member, IEEE*, Inseung Kang, *Student Member, IEEE*, Jonathan Camargo, *Student Member, IEEE*, Aaron J. Young

***Abstract*—Machine learning (ML) algorithms present an opportunity to estimate joint kinetics using a limited set of mechanical sensors. These estimates could be used as a continuous reference signal for exoskeleton control, able to modulate exoskeleton assistance in real-world environments. In this study, sagittal plane biological hip torque during level ground, incline and decline walking was calculated using inverse dynamics of human subject data. Subsequently, this torque was estimated using neural network (NN) and XGBoost ML models. Model inputs consisted solely of mechanical sensor data onboard a robotic hip exoskeleton. These results were compared to a baseline method of estimating hip torque as the mean torque profile during ambulation. On average across conditions, the NN and XGBoost models estimated biological hip torque with an RMSE of 0.116±0.015 and 0.108±0.011 Nm/kg, respectively, which was significantly less than the baseline estimation that had an RMSE of 0.300±0.145 Nm/kg ($p<0.05$). Fitting the baseline method to ambulation mode specific data significantly reduced overall RMSE by 59.3%; however, the ML models were still significantly better than the baseline method ($p<0.05$). These results show that machine learning algorithms can estimate biological hip torque using only mechanical sensors onboard a hip exoskeleton better than simply using an average torque profile. This suggests that these estimation models could be suitable for modulating exoskeleton assistance. Additionally, no evidence suggested the need to train separate ML models for each ambulation mode as estimation RMSE was not significantly different across unified and separated ML models.**

***Index Terms* – Biological Torque Estimation, Machine Learning, Regression, Exoskeleton, Ambulation**

I. Introduction

Many active hip exoskeletons have resulted in muscle-level and metabolic benefits using assistance profiles representative of or abstracted from biological joint torque [1]–[6]. Most of these successes have been limited to steady-state treadmill walking; however, many user and environmental state estimation algorithms have been developed that may be used to modulate the assistance shape and magnitude given a predefined lookup table and scaling functions [7]–[10]. Unfortunately, this approach requires many state estimates (e.g. walking speed, incline and gait phase) and predefined ambulation modes and transitions, which limits the scope and likelihood of accurate exoskeleton assistance modulation. Given these limitations, it remains unclear how well this approach would modulate bio-inspired assistance during multimodal, overground walking.

Direct estimation of biological joint torque is an alternative approach that would provide continuous estimates from a single estimator, reducing the complexity and rigidity of previous approaches. This estimate could be used as a reference signal or phase variable for an exoskeleton controller generalizable to real-world ambulation. Wearable sensors, such as inertial measurement units (IMUs), electrogoniometers and rotary encoders onboard exoskeletons, provide an alternative approach to measuring joint kinematics; however, analytical approaches to estimating biological joint torque also require measurements of external loads, such as ground reaction forces (GRFs) during the stance phase of gait. One innovative approach to this problem is the use of pressure or force sensors embedded in footwear to estimate the GRFs on the body [11]–[16]. Using these GRF measurements and wearable kinematic sensors, model-based inverse dynamics solutions can be computed without the need for external sensors, such as force plates [17]–[20]. Unfortunately, this method can be limited by the resolution of pressure insole measurements [14] and requires sensor information of distal segments and joints to estimate biological torque, resulting in complex, multi-joint measurement systems [17], [19]. Additionally, these inverse dynamics methods can be highly sensitive to anthropometric features, especially when using generalized models [17].

Machine learning (ML), along with other data-driven regression approaches, present an alternative method of estimating biomechanical measures with reduced modeling and measurement complexity [21], [22]. Jacobs and Ferris demonstrated the ability of a single-layer feedforward neural network to estimate ankle torque given various sets of wearable sensor data [11]. Howell et al. used linear regression to map pressure insole information to ankle and knee kinetics in able-bodied and post-stroke participants [16]. Additionally, Hahn and O'Keefe quantified the results of lower limb torque estimation via a feedforward neural network using demographic, anthropometric, kinematic, and electromyographic data [23]. Though these ML approaches mitigate many of the limitations of analytical model-based approaches, they still have limitations. Primarily, previous research in ML-based torque estimation often uses pressure insole measurements, maintaining the mechanical and practical limitations of such sensors [14], has been limited to simple ambulation, such as level ground walking, and often focuses on estimation of the knee and ankle joint torques, omitting biological hip torque estimation.

This gap has prompted our study to quantify the performance of biological hip torque estimation across

*This research was supported by the NSF NRI Award #1830215 and the NIH R03 Award #5R03HD097740-02. This work was also supported by the NRT: Accessibility, Rehabilitation, and Movement Science (ARMS) Award #1545287 and the Fulbright Foreign Student Fellowship.

D. D. Molinaro, I. Kang, J. Camargo, and A. J. Young are with the Institute for Robotics and Intelligent Machines (IRIM) and the Department of Mechanical Engineering, Georgia Institute of Technology, Atlanta, GA 30332 USA (e-mail: dmolinaro3@gatech.edu).

multiple ambulation modes, using a wearable sensor suite limited to those onboard a robotic hip exoskeleton (one encoder and one IMU). The sensors were integrated into the device, which provides practical benefits when considering the ease of putting on and taking off the exoskeleton compared to any additional wearable sensors. Using this data, estimation of biological hip torque was evaluated using two ML algorithms: a multi-layer feedforward neural network and the eXtreme Gradient Boosting algorithm, XGBoost [24]. The biological hip torque estimates were compared to a baseline method representative of normative hip torque profiles used as traditional inputs for bio-inspired exoskeleton control. Since these normative torque profiles have been sufficient for augmenting ambulation in controlled, steady-state environments [1]–[3], it is important that our proposed ML-based algorithms maintain or exceed this accuracy. Thus, our first hypothesis was that these ML models decrease RMSE of sagittal plane biological hip torque compared to the baseline method. Additionally, given that our method omitted direct measurement of the GRF during walking, it is likely that domain knowledge of the environment can increase the performance of each algorithm. Thus, we also hypothesized that training and testing each algorithm using ambulation mode specific data would further decrease estimated biological hip torque RMSE compared to models fit using data from all investigated ambulation modes. Therefore, our study expands on the ideas of using machine learning algorithms to improve biological torque estimation by using only exoskeleton sensors and applying these methods to various ambulation modes.

II. Methods

A. Experimental Design and Measurements

This study was approved by the Georgia Institute of Technology Institutional Review Board, and all subjects provided written informed consent for the completion of the experiment. Five able-bodied subjects (age: 23.0±2.1 years; body mass: 74.3±8.3 kg; height: 1.76±0.08 m) completed walking trials at various level ground (LG), ramp ascent (RA), and ramp descent (RD) angles of 0°, ±7.8°, ±9.2°, ±11.0°, and ±12.4°. Eight trials were completed for each slope condition, resulting in 24 LG and 32 RA and RD steady-state steps per subject for each leg (multiple steps per trial). The slope conditions were conducted in random order to remove potential bias in the hip dynamics.

Biomechanical data were collected using two methods: 1) wearable sensors onboard an autonomous robotic hip exoskeleton used as the input for the evaluated torque estimation models of this study and 2) external stationary sensors used to compute biological torque for ground truth measurements (Fig. 1). Bilateral wearable sensor data were collected using a robotic hip exoskeleton operated in zero impedance mode, which was controlled using a zero torque control reference signal regulated by a PD controller and torque measurement from series elastic actuators (SEAs) [25]. Flexion/extension hip joint angles were measured using absolute magnetic encoders (Orbis, Renishaw, UK) mounted along the axis of actuation of the exoskeleton. Additionally, six-axis acceleration and gyroscopic data were collected from IMUs (Micro USB, Yost Lab, USA) mounted on each thigh orthosis of the exoskeleton. The wearable sensor data were collected at a 100 Hz sampling frequency.

Motion capture measurements were collected at 200 Hz using a 36-camera Vicon motion capture system (Oxford Metric, Oxford, UK). GRFs were measured at 1000 Hz using Bertec force plates (Bertec, Columbus, Ohio, USA). These data were filtered using a zero-lag second order Butterworth filter with cutoff frequencies of 6 and 20 Hz, respectively. Ground truth biological hip torque was then computed using a biomechanical analysis in OpenSim v3.3 [26], [27]. Unfortunately, the exoskeleton impeded the ability to measure marker data directly attached to the biological pelvis and instead required placement of markers on the exoskeleton frame. Thus, additional care was taken to ensure appropriate scaling of the Gait2354 model used in our analysis via a two-step method. First, the model's anthropometry was scaled to that of the subject using motion capture data without wearing the exoskeleton, which included markers on the subject's left and right anterior superior iliac spine, posterior superior iliac spine, and greater trochanter. The resulting model was then scaled a second time, replacing these biological markers with those placed on the exoskeleton frame; however, the segmental properties were not updated during this second scaling operation, which only mapped the newly placed markers to the segments of the biologically scaled model. Since the exoskeleton frame fit snugly to the pelvis and upper body, the biomechanical model was simplified by adding the measured mass of the exoskeleton to the modeled torso (~8 kg). Thus, our model assumed the orientation of the exoskeleton frame aligned with that of the biological pelvis and was validated by comparing hip dynamics with and without the exoskeleton during the ambulatory tasks of this study using pilot data. Inverse kinematics and dynamics were sequentially computed using the Inverse Kinematics Tool and Inverse Dynamics Tool in OpenSim. The interaction torque between the exoskeleton and human was actively mitigated using the zero impedance control strategy, quantified to be an average of 0.25 Nm in a previous study [25], and was neglected when computing biological torque. The computed biological hip torque was normalized to the subject's body mass and filtered using a 6 Hz zero-lag second order Butterworth lowpass filter to remove discontinuities resulting from force plate contact interactions at heel strike and toe off.

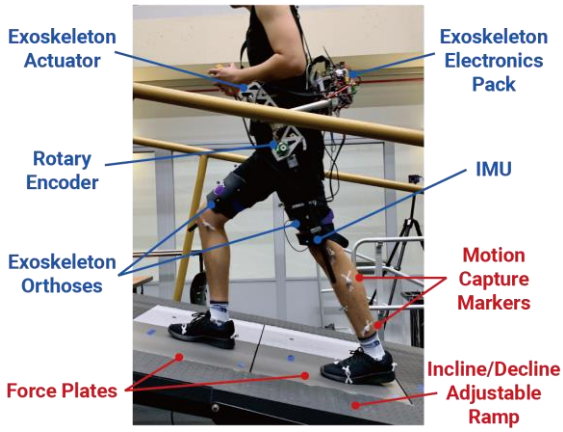

Figure 1. The experimental setup and sensors used to collect biomechanical data are shown. Blue labels denote components onboard the hip exoskeleton, and red labels are used to denote otherwise.

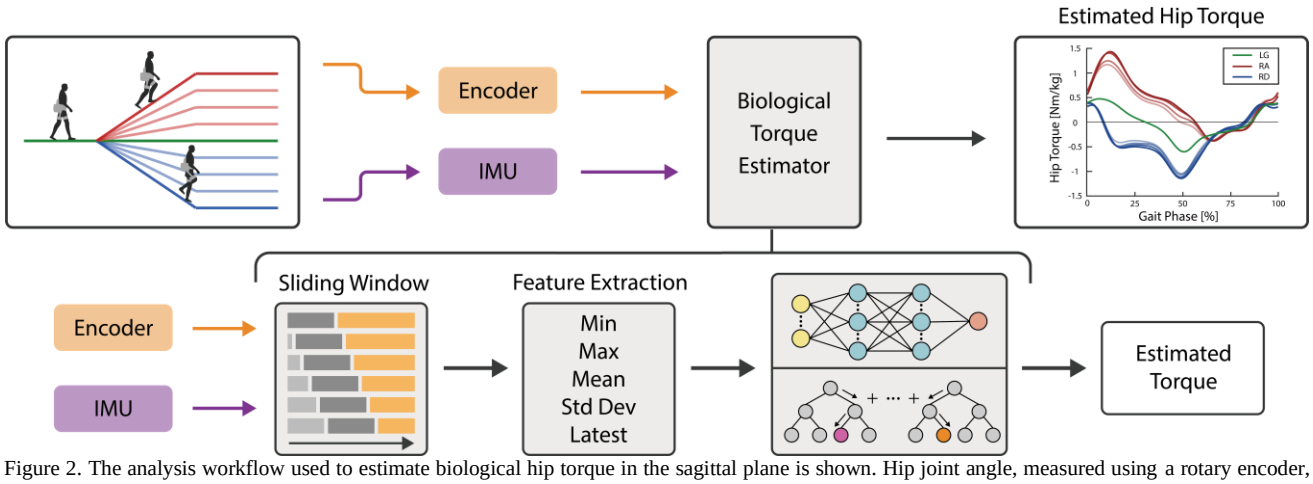

Figure 2. The analysis workflow used to estimate biological hip torque in the sagittal plane is shown. Hip joint angle, measured using a rotary encoder, and thigh acceleration and gyroscopic data, measured using an inertial measurement unit mounted on the exoskeleton thigh orthosis, are used to estimate hip torque via the biological torque estimator algorithm. This algorithm consisted of windowing the mechanical sensor data and transforming the information into several features (minimum, maximum, mean, standard deviation, and latest value). The feature data was input to one of two machine learning algorithms used in this study to estimate biological hip torque.

B. Hip Torque Estimation Algorithms

Two ML algorithms were implemented to estimate biological hip torque: a feedforward neural network (NN) and the gradient boosting algorithm, XGBoost [24]. The NN was used since similar methods have been successful in estimating joint kinematics, GRFs, and biological torque using a variety of wearable sensors [11], [21], [23]. The NN was trained and tested in Python 3.6 using Keras [28] running a TensorFlow [29] backend. The exponential linear unit (ELU) was used as the activation function given its reported fast learning benefits [30]. The number of hidden layers and nodes of the NN were determined during hyperparameter optimization (see Section II.D). A symmetric number of nodes per layer was used to limit the number of permutations of network sizes completed in our hyperparameter sweep.

XGBoost is a gradient boosting algorithm that uses unique regression trees to estimate residual error and has had success across a wide variety of regression problems [24]. We implemented this algorithm using the XGBoost module in Python 3.6. Four hyperparameters were tuned: the learning rate/shrinkage coefficient (η) used to control the influence each regression tree had on the total estimate; the minimum gain required to further split a node of the regression tree (γ); the regularization term (λ); and finally, the maximum allowed depth of each regression tree (see Section II.D).

Both torque estimation models were compared to a baseline method. The baseline method was implemented by fitting an average curve given the computed hip torque across subjects. Thus, this method predicted the average hip dynamics curve as the provided estimate, which represents the common method of determining a generic biological hip torque profile used in exoskeleton controllers [1]–[3].

C. Feature Transformation

A general workflow was developed to implement the two investigated ML algorithms for estimating biological hip torque (Fig. 2). Each hip torque estimation algorithm was trained using only the unilateral mechanical sensor data of the corresponding side of measured hip torque. The hip encoder angle, 3-axis thigh acceleration, and 3-axis thigh gyroscopic data were segmented into temporal windows and were transformed to five useful, but computationally simple features types (35 features total as inputs) containing temporal and proportional information: mean, standard deviation, minimum, maximum, and latest values [31], [32]. Bilateral feature information was omitted since our study only included symmetric, steady-state hip dynamics which is not always the case in real-world ambulation (e.g. ambulation mode transitions). Thus, including bilateral information in our study could result in overfitting of the model to symmetric gait, leading to unrealistic conclusions about estimation accuracy.

D. Algorithm Training and Testing

A test set composed of one step per leg from each ambulation condition was removed from the dataset until final testing of the tuned models. During hyperparameter tuning of each algorithm, 8-fold leave-one-step-out cross validation was used with early stopping criteria based on the rate of validation loss to prevent underfitting or overfitting of the models. Each fold of the validation set contained a single step from each ambulation mode condition. The validation dataset was the same for all hyperparameter and feature selection methods to ensure a fair comparison. Model testing consisted of a similar leave-one-step-out approach; however, each model was tested on a single step at a time to quantify test error for each ambulation mode.

Hyperparameter optimization of both machine learning algorithms was completed to ensure the model architectures were appropriate for generalizing the mechanical sensor data to biological hip torque. We implemented a directed search of unique hyperparameters for each algorithm, starting with a large sweep over the hyperparameter space. An initial window size of 250 ms was used for the first step of this search, as recommended for an ambulation mode prediction system using a similar feature set [33]. The subset of hyperparameters resulting in lowest RMSE to the validation dataset and lowest model complexity were used in a second parameter sweep, which included testing window sizes varying from 100 ms to 500 ms in increments of 50 ms. The resulting set of hyperparameters and window size that

minimized RMSE while limiting model complexity (i.e. hidden nodes/layers and maximum tree depth) and window size was then selected using the elbow method for all later analyses [34]. The selected NN hyperparameters were three hidden layers, 30 nodes per layer, and a 350 ms window. The selected XGBoost hyperparameters were maximum tree depth of 6, η of 0.05, γ of 0, λ of 1, and a 350 ms window.

Using these selected hyperparameters, sequential forward feature-type (mean, std., min., max., latest) selection and sequential forward channel-type (encoder angle, accel x-y-z, gyro x-y-z) selection were run using both machine learning algorithms to remove less relevant features and mitigate the "curse of dimensionality" [35]. Feature-type selection of both the NN and XGBoost methods resulted in minimum RMSE using only mean, standard deviation, and latest value feature types. Thus, the minimum and maximum feature types were removed from all further analyses. Channel-type selection was also run both before and after feature-type selection for both algorithms. Minimum RMSE was achieved by using all available sensor channels for both algorithms.

E. Ambulation Mode Dependency

Ambulation mode dependent and independent methods were used when fitting the ML and baseline models. These two conditions represent a premise in which the ambulation mode is known or unknown to the exoskeleton, respectively, which provides insight into the need of ambulation mode classification algorithms when implementing these estimators during real-world ambulation. The mode dependent condition was completed by training and testing individual models and baseline torque profiles for each ambulation mode (LG, RA, RD). In contrast, the mode independent condition used unified ML models and a baseline torque profile regardless of ambulation mode.

F. Statistical Analysis

A two-way repeated measures analysis of variance (ANOVA) was used to determine significant differences within and between the hip torque estimation algorithms and ambulation mode dependence using a 0.05 alpha level of significance. A *post hoc* multiple comparisons test using a Bonferroni-correction was used to compute statistical differences between each condition. SPSS Statistics 21.0 (IBM, Amonk, NY, USA) was used for all statistical tests.

III. Results

A. Algorithm Performance

There were no statistical differences in estimated hip torque RMSE between the NN and XGBoost models (Fig. 3). When trained using the mode independent method, the XGBoost algorithm reduced estimated hip torque RMSE by 73.3±4.5%, 38.4±30.8%, 77.3±2.9%, and 71.7±7.6% compared to the baseline method for the aggregate, LG, RA, and RD results, respectively. Similarly, when trained using the mode dependent method, the XGBoost algorithm reduced RMSE by 39.3±5.0%, 43.2±23.1%, 48.1±4.5%, and 26.6±11.1% relative to the baseline method for the aggregate, LG, RA, and RD results, respectively. These reductions in error were significant for all pairwise comparisons except for those of the LG results ($p<0.05$). Comparing the NN hip torque to the baseline method yielded similar statistical comparisons, other than the mode dependent RD result ($p<0.05$) (Fig. 3d).

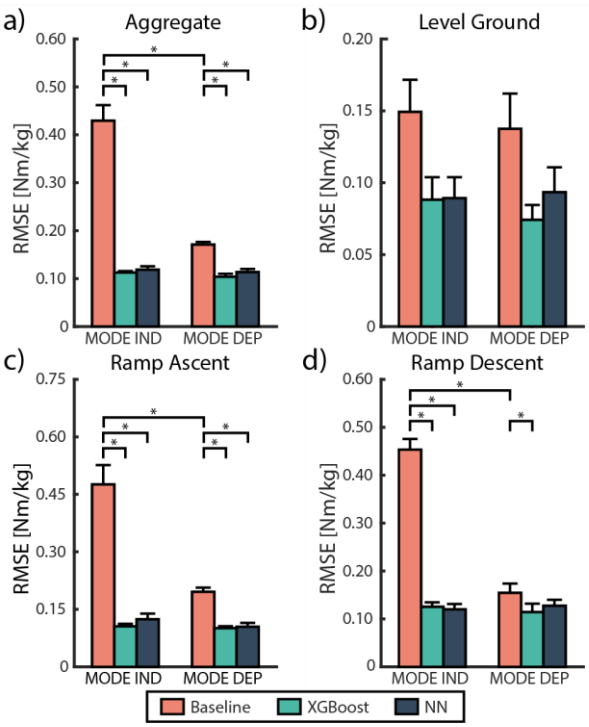

Figure 3. Performance of the hip torque estimation algorithms are shown as the average RMSE across all ambulation modes (a), and per ambulation mode for level ground (b), ramp ascent (c), and ramp descent (d) walking. Results are presented for the baseline, XGBoost, and neural network (NN) estimation methods and when trained using the mode independent (MODE IND) and mode dependent (MODE DEP) paradigms. Error bars represent +1 standard error of the mean. * indicates statistical significance ($p<0.05$).

B. Ambulation Mode Dependency Comparison

Training the XGBoost and NN models with ambulation mode dependency compared to the mode independent method did not result in a significant difference in hip torque estimation RMSE (Fig. 3). Unlike the machine learning methods, fitting the baseline method with ambulation mode specific data significantly reduced RMSE by 59.3±7.8%, 57.4±9.9%, and 64.8±14.3% for the aggregate, RA, and RD results, respectively ($p<0.05$). Mode dependency did not result in significantly different RMSE when fitting the baseline method for the LG result given the similarity in LG hip torque compared to the averaged hip torque across ambulation modes (Fig. 4).

IV. Discussion

Our study presented a novel method of estimating biological hip torque during multiple ambulation modes using only mechanical sensors onboard an autonomous hip exoskeleton. In general, we accepted our hypothesis that using machine learning algorithms with mechanical sensor inputs would improve the estimation of biological hip torque compared to the baseline method. LG ambulation was the only ambulation mode in which the ML models did not significantly improve torque tracking, despite an average reduction in hip torque RMSE of 38%. This was likely due to

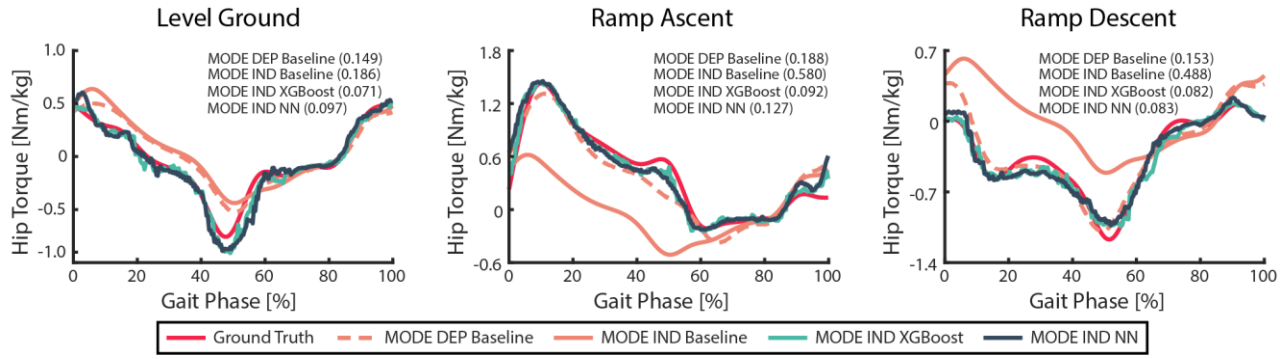

Figure 4. Ground truth biological hip torque of a single step for each ambulation mode is shown alongside the estimates using the mode independent (MODE IND) and mode dependent (MODE DEP) baseline method and the MODE IND XGBoost and neural network (NN) models. The single-step RMSE for each method compared to the ground truth curve is shown in parentheses. Ramp ascent and descent data are shown for the 12.4° slope.

the low variance in hip dynamics exhibited during steady-state LG walking and the limited participant size of this study (N=5). These results promote the use of ML-based torque estimation to reduce the complexity and error in estimating hip torque using wearable sensors.

We also hypothesized that training unique models for each ambulation mode (LG, RA, RD) would further improve hip torque estimation by reducing the system domain. As expected, the baseline method improved when fit using ambulation mode specific data. This was expected as hip torque profiles vary given different ambulation modes (Fig. 4). Thus, if using the baseline method to estimate biological hip torque during level ground and slope walking, ambulation mode should be used to delineate estimated profiles, requiring additional state estimators, such as an ambulation mode classifier [8], [10], [32], [33]. Unlike the baseline result, the XGBoost and NN algorithms resulted in no significant difference when comparing ambulation mode dependent and independent models and overall RMSE below 0.119 Nm/kg regardless of ambulation mode dependency. This suggests that these algorithms were able to appropriately generalize the input feature space to hip torque estimation regardless of known ambulation mode.

Additionally, the error in hip torque estimation of our study is favorable when compared to those computed using other methods. Forner-Cordero et al. reported hip torque estimation RMSE of approximately 0.15 Nm/kg using a pressure insole informed inverse dynamics approach during level ground walking [18]. In comparison, the average RMSE of estimated hip torque during level ground walking in our study was below 0.093 Nm/kg, regardless of ML algorithm and mode dependency. Hahn and O'Keefe presented a method of estimating biological hip torque using a feedforward neural network trained using combinations of several datatypes [23]. This method resulted in sagittal plane hip torque estimation RMSE of 0.20 Nm/kg, which was also larger than the comparable RMSE reported in our study. Additionally, assuming our reported RMSE of 0.093 Nm/kg during LG walking altered the estimated biological peak torque by this magnitude, it can be inferred that the metabolic benefit compared to unpowered walking reported in [5] would be altered from 6% to approximately 5.8%. Future research using these algorithms to modulate exoskeleton control online is needed since there are many confounding factors that may influence this prediction; however, this suggests that the estimation errors found in our study may be sufficiently low for exoskeleton control.

One limitation of this study is that all ambulation data used for training and testing the algorithms were representative of steady-state locomotion. Conventionally, estimation of user state is often more challenging during transient locomotion, such as when turning during ambulation and transitioning between modes [32]. Thus, future analyses should investigate the ability of ML algorithms to estimate biological joint moments during transient ambulation. Similarly, it is possible that the model would need to be retrained to estimate joint torque during active exoskeleton assistance conditions due to the expected changes in biological joint kinematics and soft tissue deformation between the orthosis and wearer. Future research should investigate the robustness of this algorithm to assistance conditions. Additionally, the output of the trained ML algorithms was not smooth (Fig. 4) since no temporal relationship was enforced for the output of the ML models. This could cause instability if using raw model output for exoskeleton control and suggests the need for additional filtering techniques or sequence models.

Another limitation of our study is that the machine learning models were trained on user specific data. This method of collecting training data is impractical as the initial biological hip torque data used to train the models required substantial processing for each subject. Given the repeatability of mechanical sensor data across subjects, it is likely that unified, user independent models can be trained that would not require individual subject data to estimate biological joint torque. Given the limited participant size, this analysis was outside the scope of our study, but presents an exciting opportunity to remove the burden of user specific model training. As such, the limited participant size (N=5) is another limitation of this study, suggesting the need for more subjects to further power our analysis.

V. Conclusion

Our study compared machine learning-based biological hip torque estimators informed by mechanical measurements onboard a robotic hip exoskeleton to a baseline method and to results of similar studies in the literature. The machine learning-based methods reduced estimated hip torque RMSE beyond the baseline method and reported literature values. Thus, hip torque estimation approaches using machine

learning are a viable method for accurate estimation. Additionally, the machine learning models were able to appropriately generalize to multiple ambulation modes and slopes regardless of ambulation mode dependent or independent training. This validates our method as a novel approach to estimating hip kinetics across ambulation modes without the need for additional domain knowledge.

ACKNOWLEDGMENT

We would like to thank Julian Park, Henry Luk, and Gayeon Choi for their help in data collection for this study.

REFERENCES

[1] K. Seo, J. Lee, Y. Lee, T. Ha, and Y. Shim, "Fully autonomous hip exoskeleton saves metabolic cost of walking," in *2016 IEEE International Conference on Robotics and Automation (ICRA)*, 2016, pp. 4628–4635.

[2] K. Seo, J. Lee, and Y. J. Park, "Autonomous hip exoskeleton saves metabolic cost of walking uphill," in *2017 International Conference on Rehabilitation Robotics (ICORR)*, 2017, pp. 246–251.

[3] T. Lenzi, M. C. Carrozza, and S. K. Agrawal, "Powered hip exoskeletons can reduce the user's hip and ankle muscle activations during walking," *IEEE Transactions on Neural Systems and Rehabilitation Engineering*, vol. 21, no. 6, pp. 938–948, 2013.

[4] Y. Ding *et al.*, "Effect of timing of hip extension assistance during loaded walking with a soft exosuit," *Journal of neuroengineering and rehabilitation*, vol. 13, no. 1, p. 87, 2016.

[5] I. Kang, H. Hsu, and A. Young, "The effect of hip assistance levels on human energetic cost using robotic hip exoskeletons," *IEEE Robotics and Automation Letters*, vol. 4, no. 2, pp. 430–437, 2019.

[6] F. Giovacchini *et al.*, "A light-weight active orthosis for hip movement assistance," *Robotics and Autonomous Systems*, vol. 73, pp. 123–134, 2015.

[7] Q. Li, M. Young, V. Naing, and J. M. Donelan, "Walking speed and slope estimation using shank-mounted inertial measurement units," in *2009 IEEE International Conference on Rehabilitation Robotics*, 2009, pp. 839–844.

[8] J. Jang, K. Kim, J. Lee, B. Lim, and Y. Shim, "Online gait task recognition algorithm for hip exoskeleton," in *2015 IEEE/RSJ International Conference on Intelligent Robots and Systems (IROS)*, 2015, pp. 5327–5332.

[9] I. Kang, P. Kunapuli, and A. J. Young, "Real-Time Neural Network-Based Gait Phase Estimation using a Robotic Hip Exoskeleton," *IEEE Transactions on Medical Robotics and Bionics*, 2019.

[10] K. Yuan *et al.*, "A realtime locomotion mode recognition method for an active pelvis orthosis," in *2015 IEEE/RSJ International Conference on Intelligent Robots and Systems (IROS)*, 2015, pp. 6196–6201.

[11] D. A. Jacobs and D. P. Ferris, "Estimation of ground reaction forces and ankle moment with multiple, low-cost sensors," *J NeuroEngineering Rehabil*, vol. 12, no. 1, p. 90, Dec. 2015, doi: 10.1186/s12984-015-0081-x.

[12] D. T.-P. Fong, Y.-Y. Chan, Y. Hong, P. S.-H. Yung, K.-Y. Fung, and K.-M. Chan, "Estimating the complete ground reaction forces with pressure insoles in walking," *Journal of Biomechanics*, vol. 41, no. 11, pp. 2597–2601, Aug. 2008, doi: 10.1016/j.jbiomech.2008.05.007.

[13] M. Hirasawa, H. Okada, and M. Shimojo, "The development of the plantar pressure sensor shoes for gait analysis," *Journal of Robotics and Mechatronics*, vol. 20, no. 2, p. 289, 2008.

[14] A. Razak, A. Hadi, A. Zayegh, R. K. Begg, and Y. Wahab, "Foot plantar pressure measurement system: A review," *Sensors*, vol. 12, no. 7, pp. 9884–9912, 2012.

[15] A. Forner Cordero, H. J. F. M. Koopman, and F. C. T. van der Helm, "Use of pressure insoles to calculate the complete ground reaction forces," *Journal of Biomechanics*, vol. 37, no. 9, pp. 1427–1432, Sep. 2004, doi: 10.1016/j.jbiomech.2003.12.016.

[16] A. M. Howell, T. Kobayashi, H. A. Hayes, K. B. Foreman, and S. J. M. Bamberg, "Kinetic Gait Analysis Using a Low-Cost Insole," *IEEE Transactions on Biomedical Engineering*, vol. 60, no. 12, pp. 3284–3290, Dec. 2013, doi: 10.1109/TBME.2013.2250972.

[17] B. Hwang and D. Jeon, "Estimation of the User's Muscular Torque for an Over-ground Gait Rehabilitation Robot Using Torque and Insole Pressure Sensors," *Int. J. Control Autom. Syst.*, vol. 16, no. 1, pp. 275–283, Feb. 2018, doi: 10.1007/s12555-016-0545-1.

[18] A. Forner-Cordero, H. J. F. M. Koopman, and F. C. T. van der Helm, "Inverse dynamics calculations during gait with restricted ground reaction force information from pressure insoles," *Gait & Posture*, vol. 23, no. 2, pp. 189–199, Feb. 2006, doi: 10.1016/j.gaitpost.2005.02.002.

[19] K. Kanjanapas and M. Tomizuka, "7 Degrees of Freedom Passive Exoskeleton for Human Gait Analysis: Human Joint Motion Sensing and Torque Estimation During Walking," *IFAC Proceedings Volumes*, vol. 46, no. 5, pp. 285–292, 2013.

[20] J. Bae, K. Kong, and M. Tomizuka, "Real-time estimation of lower extremity joint torques in normal gait," *IFAC Proceedings Volumes*, vol. 42, no. 16, pp. 443–448, 2009.

[21] A. Ancillao, S. Tedesco, J. Barton, and B. O'Flynn, "Indirect measurement of ground reaction forces and moments by means of wearable inertial sensors: A systematic review," *Sensors*, vol. 18, no. 8, p. 2564, 2018.

[22] R. D. Gurchiek, N. Cheney, and R. S. McGinnis, "Estimating Biomechanical Time-Series with Wearable Sensors: A Systematic Review of Machine Learning Techniques," *Sensors*, vol. 19, no. 23, p. 5227, 2019.

[23] M. E. Hahn and K. B. O'Keefe, "A neural network model for estimation of net joint moments during normal gait," *Journal of Musculoskeletal Research*, vol. 11, no. 03, pp. 117–126, 2008.

[24] T. Chen and C. Guestrin, "Xgboost: A scalable tree boosting system," in *Proceedings of the 22nd acm sigkdd international conference on knowledge discovery and data mining*, 2016, pp. 785–794.

[25] I. Kang, P. Kunapuli, H. Hsu, and A. J. Young, "Electromyography (EMG) Signal Contributions in Speed and Slope Estimation Using Robotic Exoskeletons," in *2019 IEEE 16th International Conference on Rehabilitation Robotics (ICORR)*, Jun. 2019, pp. 548–553, doi: 10.1109/ICORR.2019.8779433.

[26] S. L. Delp *et al.*, "OpenSim: open-source software to create and analyze dynamic simulations of movement," *IEEE transactions on biomedical engineering*, vol. 54, no. 11, pp. 1940–1950, 2007.

[27] A. Seth *et al.*, "OpenSim: Simulating musculoskeletal dynamics and neuromuscular control to study human and animal movement," *PLoS computational biology*, vol. 14, no. 7, p. e1006223, 2018.

[28] F. Chollet, *keras*. 2015.

[29] M. Abadi *et al.*, "TensorFlow: A System for Large-Scale Machine Learning," presented at the 12th {USENIX} Symposium on Operating Systems Design and Implementation ({OSDI} 16), 2016, pp. 265–283, Accessed: Feb. 05, 2020. [Online]. Available: https://www.usenix.org/conference/osdi16/technical-sessions/presentation/abadi.

[30] D.-A. Clevert, T. Unterthiner, and S. Hochreiter, "Fast and Accurate Deep Network Learning by Exponential Linear Units (ELUs)," *arXiv:1511.07289 [cs]*, Feb. 2016, Accessed: Feb. 05, 2020. [Online]. Available: http://arxiv.org/abs/1511.07289.

[31] H. A. Varol, F. Sup, and M. Goldfarb*, "Multiclass Real-Time Intent Recognition of a Powered Lower Limb Prosthesis," *IEEE Transactions on Biomedical Engineering*, vol. 57, no. 3, pp. 542–551, Mar. 2010, doi: 10.1109/TBME.2009.2034734.

[32] A. J. Young, A. M. Simon, N. P. Fey, and L. J. Hargrove, "Intent Recognition in a Powered Lower Limb Prosthesis Using Time History Information," *Ann Biomed Eng*, vol. 42, no. 3, pp. 631–641, Mar. 2014, doi: 10.1007/s10439-013-0909-0.

[33] A. J. Young, A. M. Simon, and L. J. Hargrove, "A Training Method for Locomotion Mode Prediction Using Powered Lower Limb Prostheses," *IEEE Transactions on Neural Systems and Rehabilitation Engineering*, vol. 22, no. 3, pp. 671–677, May 2014, doi: 10.1109/TNSRE.2013.2285101.

[34] P. Bholowalia and A. Kumar, "EBK-means: A clustering technique based on elbow method and k-means in WSN," *International Journal of Computer Applications*, vol. 105, no. 9, 2014.

[35] R. Bellman, "Dynamic Programming," *Science*, vol. 153, no. 3731, pp. 34–37, Jul. 1966, doi: 10.1126/science.153.3731.34.